

# Exploring Sparse Representation Measures of Physiological Synchrony for Romantic Couples

Theodora Chaspari\*, Adela C. Timmons\*, Brian R. Baucom<sup>†</sup>, Laura Perrone<sup>‡</sup>, Katherine J.W. Baucom<sup>†</sup>, Panayiotis Georgiou\*, Gayla Margolin\* and Shrikanth S. Narayanan\*

\*University of Southern California

<sup>†</sup>University of Utah

<sup>‡</sup>Stony Brook University

**Abstract**—Quantifying the inherent coordination between interacting individuals can afford us new insights into their emotions, communicative intent, and relationship quality. We propose a novel framework to capture the physiological synchrony between romantic partners through sparse representation techniques and appropriately designed parametric dictionaries that take into account the characteristic structure of the considered signals. Physiological synchrony is operationalized as the similarity of co-occurring electrodermal activity (EDA) streams captured through the distance in the corresponding parametric representation space, as well as through the joint signal representation errors. Results indicate that the proposed sparse EDA synchrony measures (SESM)—evaluated on two datasets of couples’ interactions—differ across tasks of various emotional intensity and are associated with the partners’ attachment style. These results provide a foundation towards designing novel descriptors of interaction and physiological linkage between individuals for emerging affective computing applications.

## 1. Introduction

Interpersonal synchrony refers to the temporal coordination of behaviors between individuals. This inherent tendency to co-regulate has been extensively studied in relation to social, psychological, and developmental factors [1], [2]. Beyond the behavioral level, life-science researchers have also examined co-regulation of physiological patterns between individuals focusing on patient-therapist, child-parent, and romantic relations [3], [4], [5]. Both risks and benefits have been associated with the presence of this physiological linkage depending on the context, nature of interaction and individual characteristics [6].

A variety of studies have established the existence of physiological synchrony between romantic couples as part of a framework that examines the general interplay of partners’ mood, emotions, and physiology [7], [8], [9], [10]. This phenomenon is of special interest to researchers since the extent to which one’s behavior affects his/her partner has implications related not only to the functioning of the relationship, but also to the individuals’ health and well-being [4], [6], [11]. Devising novel ways to reliably quantify

this physiological coordination is an important building block for assisting and further advancing these studies.

Previous work has proposed a variety of signal processing and time-series analyses in order to capture physiological synchrony. Statistical approaches involve the use of bivariate time-series and multilevel models [7], [12]. Dynamical systems have been introduced as an intuitive way to quantify an individual’s self-regulation and partners’ co-regulation through the parameters of a coupled linear oscillator [8], [9], [13]. Interpersonal synchrony has also been modeled through (cross-lagged) correlation, recurrence analysis, and spectral coherence [14], [15]. A detailed review of these approaches can be found in [16]. These mathematical models have shown a great promise for quantifying the linkage in terms of behavioral and physiological patterns. However, they typically capture the coordination of aggregated measures derived from the signals of interest rather than the co-evolution between the signal trends and fluctuations. To overcome this issue, we propose an alternative way to quantify this bio-linkage by measuring the similarity of the original physiological signals rather than the summary measures derived from those.

Many biomedical signals depict a characteristic structure over time that can be taken into account when designing physiological models. Previous studies have proposed signal-specific parametric dictionaries with the use of sparse representation techniques in order to represent and interpret physiological signals, such as the electrodermal activity (EDA) and the electrocardiogram (ECG) [17], [18]. These models incorporate the main information into a carefully-designed parametric space, whose parameters depict the morphology (e.g. fluctuations, amplitude, etc.) of the considered data. Multidimensional sparse representation techniques have been employed to jointly represent parallel streams of data and evaluate their similarity [17].

In the current paper, we extend this signal similarity index to a variety of synchrony scores derived from the distance metrics of the corresponding parametric spaces. We further introduce symmetric and asymmetric synchrony indices through the joint representation error of the two signals (Section 2). Our approach is exemplified for the EDA, while similar methods can be applied to any signal of characteristic structure. We evaluate the proposed sparse

EDA synchrony measures (SESM) on two datasets that include interactions of romantic couples (Section 3) and examine those measures in relation to tasks of various emotional intensity, as well as in association to partners' relationship attachment style (Section 4). Results indicate that the SESM scores significantly vary across the different tasks and can predict avoidance and anxiety indices with moderate correlation when used in a non-linear regression framework (Section 5). These are consistent with previous findings [7], [12] supporting the feasibility of the proposed approach for quantifying EDA synchrony.

## 2. Sparse EDA Synchrony Measures (SESM)

EDA is typically decomposed into the tonic part or skin conductance level (SCL), which refers the signal trends, and the phasic part or skin conductance responses (SCR), which are the fluctuations superimposed onto the tonic signal. The latter usually depicts an abrupt increase and slow recovery, properties which can be captured through appropriately designed parametric functions. These parametric functions can serve as the basis of EDA-specific dictionaries in the framework of sparse representation techniques [17].

We will briefly describe the sparse representation of a single EDA signal with appropriately designed dictionaries and demonstrate how the parameters of this model can be used to derive distance metrics capturing the similarity between two signals (Section 2.1). We will further discuss how this can be extended to a joint sparse representation framework that results in symmetric and asymmetric synchrony indices of two EDA signals (Section 2.2).

### 2.1. Single-Representation SESM

An EDA signal  $\mathbf{f} \in \mathbb{R}^L$  can be expressed as a linear combination of a small number of parametric atoms from a dictionary  $\mathbf{D} \in \mathbb{R}^{L \times K}$ . The dictionary contains tonic and phasic atoms captured with straight lines and Bateman functions written as follows:

$$g_{tonic}(t) = \Delta_0 + \Delta \cdot t \quad (1)$$

$$g_{phasic}(t) = \left( e^{-a(st-t_0)} - e^{-b(st-t_0)} \right) u(t-t_0) \quad (2)$$

where  $\Delta_0 \in \{-20, -10, 1\}$  and  $\Delta \in \{-0.010, -0.009, \dots, -0.001, 0, 0.01, 0.02, \dots, 0.10\}$  are the offset and slope of the tonic atoms, and  $a \in \{0.2, 0.6, 1, 1.4\}$ ,  $b \in \{0.4, 0.8, 1.2, 1.6\}$ ,  $s \in \{0.02, 0.04, \dots, 0.14\}$ ,  $t_0 \in \{0, 10, \dots, 610\}$  are the steepness of recovery, steepness of onset, time scale and time shift of the phasic atoms.

Sparse decomposition is performed using the orthogonal matching pursuit (OMP) [19], [20] because of its efficiency and theoretical guarantees of correctness [21], [22]. According to this, a signal  $\mathbf{f}$  can be approximated as  $\mathbf{f} \approx \mathbf{D}_N \cdot \mathbf{c}$ , where  $\mathbf{D}_N \in \mathbb{R}^{L \times N}$  includes only the small set of atoms ( $N \ll K$ ) selected from OMP and  $\mathbf{c} \in \mathbb{R}^N$  represents the vector of corresponding atom coefficients. Let  $\Phi_{N'} = [\phi_1 \dots \phi_{N'}] \in \mathbb{R}^{4 \times N'}$  be the matrix containing

the parameters of the selected phasic atoms, where each vector  $\phi_n \in \mathbb{R}^4$  includes the corresponding steepness of onset, steepness of recovery, time scale and time shift. Since the representation of an EDA signal also typically contains tonic atoms, we denote the number of phasic atoms  $N'$  differently from the total number of selected atoms  $N$  ( $N' < N$ ). Moreover, EDA fluctuations have been widely associated with various psychophysiological conditions [23], [24], thus we give emphasis on the phasic part of the signal when designing the synchrony indices.

Hence, through sparse decomposition we can represent two EDA signals as  $\mathbf{f}_1 \approx \mathbf{D}_{N1} \cdot \mathbf{c}_1$  and  $\mathbf{f}_2 \approx \mathbf{D}_{N2} \cdot \mathbf{c}_2$ , where  $\mathbf{D}_{N1}, \mathbf{D}_{N2} \in \mathbb{R}^{L \times N}$  are the atoms independently selected for the first and second EDA signals through OMP,  $\mathbf{c}_1, \mathbf{c}_2 \in \mathbb{R}^N$  are the corresponding coefficients. Let  $\Phi_{N1'} \in \mathbb{R}^{4 \times N1'}$ ,  $\Phi_{N2'} \in \mathbb{R}^{4 \times N2'}$  be the matrices including the parameters of the selected phasic atoms and  $\mathbf{c}'_1 \in \mathbb{R}^{N1'}$ ,  $\mathbf{c}'_2 \in \mathbb{R}^{N2'}$  be the coefficients corresponding to these phasic atoms ( $N1', N2' < N$ ). We define the distance metrics between the two signals with respect to their parametric representation space augmented by the corresponding coefficients as follows:

$$D_{DTW} = \frac{1}{\max(N1', N2')} \text{DTW}([\Phi_{N1'}; \mathbf{c}'_1], [\Phi_{N2'}; \mathbf{c}'_2]) \quad (3)$$

$$D_{L2} = \frac{1}{\min(N1', N2')} \|\Phi_{N1'}; \mathbf{c}'_1 - \Phi_{N2'}; \mathbf{c}'_2\|_2 \quad (4)$$

where DTW is the similarity measure yielding from the dynamic time warping between two multidimensional sequences and  $\|\cdot\|_2$  is the  $l_2$ -norm between two matrices. In the above equations, each matrix  $[\Phi_{Nm'}; \mathbf{c}'_m]$  ( $m=1,2$ ) is normalized so that the values of its elements range between 0 and 1. During the computation of  $D_{L2}$ , if the two EDA signals are captured by different number of phasic atoms, we omit the ones with the smallest coefficients from the representation with the excessive atoms. Based on these distance metrics, we can further derive the single-representation synchrony indices as:

$$\text{S-SESM}_{DTW} = 1 - D_{DTW} \quad (5)$$

$$\text{S-SESM}_{L2} = 1 - D_{L2} \quad (6)$$

The aforementioned  $l_2$ -norm can be computed for each of the parameters and coefficients of the phasic atoms separately as distance between vectors rather than matrices, i.e.  $1 - \frac{1}{\min(N1', N2')} \|\mathbf{c}'_1 - \mathbf{c}'_2\|_2$ , etc.

### 2.2. Joint-Representation SESM

An alternative approach would be to jointly represent two EDA streams through a common set of atoms from the dictionary. This can be performed using the simultaneous orthogonal matching pursuit (SOMP) [25], according to which two signals can be expressed as  $\mathbf{f}_1 \approx \mathbf{D}_N \cdot \mathbf{c}_1$  and  $\mathbf{f}_2 \approx \mathbf{D}_N \cdot \mathbf{c}_2$ , where  $\mathbf{D}_N \in \mathbb{R}^{L \times N}$  includes the atoms jointly selected for both signals through SOMP and  $\mathbf{c}_1, \mathbf{c}_2$  the corresponding coefficients computed for each signal.

Intuitively, if the signals  $\mathbf{f}_1$  and  $\mathbf{f}_2$  are similar to each other, the common atoms selected through SOMP can reliably capture their structure, resulting in low representation error. We can express the synchrony measure between the two signals as the negative logarithm of their joint representation error as follows:

$$\text{J-SESM} = -\log \left[ \frac{1}{2} \left( \frac{\|\mathbf{f}_1 - \tilde{\mathbf{f}}_1\|_2}{\|\mathbf{f}_1\|_2} + \frac{\|\mathbf{f}_2 - \tilde{\mathbf{f}}_2\|_2}{\|\mathbf{f}_2\|_2} \right) \right] \quad (7)$$

where  $\tilde{\mathbf{f}}_1$  and  $\tilde{\mathbf{f}}_2$  are the reconstructed signals. This expression includes the normalized representation error (ranging between 0 and 1), while the logarithmic scaling helps reducing the skewness towards values of the error closer to 1. More details on this approach can be found in [26].

In order to incorporate a sense of directionality in the proposed synchrony measure, we further propose asymmetric indices that capture the extent to which components of one signal can be reliably used to represent the other. Let  $\mathbf{D}_{N1}$ ,  $\mathbf{D}_{N2}$  be the atoms selected for the first and second EDA signals independently through OMP. In order to capture these asymmetric effects, we can use the atoms selected for the first signal as a basis to decompose the second and vice-versa, i.e.  $\tilde{\mathbf{f}}_{12} = \mathbf{D}_{N2} \cdot \mathbf{c}_1$  and  $\tilde{\mathbf{f}}_{21} = \mathbf{D}_{N1} \cdot \mathbf{c}_2$ . The asymmetric synchrony scores, denoted as  $\text{J-SESM}_{12}$  and  $\text{J-SESM}_{21}$ , can be computed as the negative logarithm of the corresponding representation errors:

$$\text{J-SESM}_{12} = -\log \left( \frac{\|\mathbf{f}_1 - \tilde{\mathbf{f}}_{12}\|_2}{\|\mathbf{f}_1\|_2} \right) \quad (8)$$

$$\text{J-SESM}_{21} = -\log \left( \frac{\|\mathbf{f}_2 - \tilde{\mathbf{f}}_{21}\|_2}{\|\mathbf{f}_2\|_2} \right) \quad (9)$$

Intuitively we understand that index  $\text{J-SESM}_{12}$  depicts how well the first EDA signal matches the structure of the second, and similarly for  $\text{J-SESM}_{21}$ .

### 3. Data Description

We examine two datasets that contain interactions of couples from in-lab visits. Both experimental procedures include relaxation tasks to establish physiological baseline, as well as neutral and emotionally intense discussions. EDA signals were recorded with the Biopac MP150 system at a sampling rate of 62.5Hz.

The first dataset (referred as *Young Couples' Interactions*) includes 35 young-adult dating couples (ages 18-25). A large portion of the participants were recruited as a part of a longitudinal study, during which they had come to the lab as teens. First the couples were introduced to a 10min *Relaxation* task, during which they watched a soothing video while sitting. Then they engaged in a 5-min *Date Planning* discussion in which they had to arrange a potential future date. More emotionally intense tasks included the *Change* discussion, in which the participants talked about what they would like to change in their relationship, and two loss discussions in which the female (*LossF*) and male (*LossM*)

partners described a significant loss in their lives. Each one of these discussions lasted for 10 mins.

The second dataset (referred as *Married Couples' Interactions*) includes 30 married couples (ages 21-47) participating in a larger study of emotion and behavior. Couples were first asked to sit quietly in separate rooms (*BaselineS*) and at the same room (*BaselineT*). Each of these relaxation periods lasted 5 mins. Afterwards they engaged in a casual discussion (5 mins) in which they had to describe to each other the main events of their day (*Events*). More emotionally intense tasks include two discussions (10 mins each) during which couples talked about the things that the wife (*ChangeW*) and the husband (*ChangeH*) wanted to change in their marriage. Finally participants were asked to discuss the beginning of their relationship (*History*) for 7.5 mins, which served as a recovery task.

Participants completed self-reports of attachment style, in order to get a measure of how they relate to their partner. Attachment is typically described by two orthogonal dimensions of avoidance and anxiety. Avoidant individuals depict the tendency to withdraw from closeness and intimacy, while anxious individuals tend to feel insecure and have conflicted thoughts and feelings about their romantic partners. Attachment was measured through the *Experiences in Close Relationships-Revised (ECR-R)* [27] and the *Adult Attachment Questionnaire (AAQ)* [28] for the young and married couples, respectively. For our analysis, avoidance and anxiety scores were averaged across the two partners yielding couple-specific attachment descriptors.

### 4. Contextualizing EDA Synchrony

Contextualizing and interpreting physiological synchrony is a challenging problem, since it is difficult to determine the ground truth. Taking this into account, synchrony measures are often indirectly evaluated depending on the application of interest. We will demonstrate two ways to assess the usefulness of the proposed SESM indices specific to the domain of our data. We also will examine how synchrony varies depending on the emotional intensity of the task, as well as its association to couples' attachment style.

The tasks included in the considered experimental procedures (Section 3) elicit various emotional responses that can result in different physiological reactivity and therefore distinct synchrony patterns [7]. We examine if there are significant differences among the group means of the proposed synchrony measures across tasks through analysis of variance (ANOVA).

Previous studies have indicated that increased EDA reactivity in couples has been related to both anxiously and avoidantly attached individuals, since the former seeks increased connection, while the latter avoids connection with others [12]. Based on these findings, we evaluate the proposed SESM in relation to the couples' self-reported attachment.

We first compute the Pearson's correlation coefficient between each synchrony index and the anxiety and avoidance

scores. Next we develop a machine learning framework to predict the attachment ratings using the synchrony measures as features of the system. A deep neural network (DNN) architecture is employed to simulate a non-linear regression function (Fig. 1). The input features included the S-SESM and J-SESM scores, as defined in (5)-(9). We further added to this vector the  $l_2$ -norm of each of the phasic atom parameters, as well as the  $l_2$ -norm of the corresponding coefficients (as described in Section 2.1). This results in a feature vector  $\mathbf{x} \in \mathbb{R}^d$  with  $d=7$  input attributes for the S-SESM,  $d=3$  for the J-SESM, and  $d=10$  when we include both. The feature input is followed by two fully connected feed-forward layers, one with the same number of neurons as the input attributes (i.e.  $d$ ) and the next with half the number of neurons (i.e.  $\lfloor d/2 \rfloor$ ), both employing the hyperbolic tangent as an activation function. The output is a linear layer with no activation function, since we are interested in directly predicting the avoidance and anxiety values as a 2-dimensional vector. The system was trained in 100 epochs using the ADAM algorithm [29] and a mean square error loss function as an optimization criterion. A 5-fold cross-validation setup is employed, during which no data from the same couple were simultaneously available during training and testing. The Keras implementation [30] was used with the Theano toolbox [31] as the back-end.

## 5. Results

EDA representation was performed with a 10 sec analysis window, 5 OMP and SOMP iterations. Previous studies suggest that this time frame incorporates enough signal variability, but also preserves computationally tractable implementations [17]. The dictionary contained 63 tonic and 4340 phasic atoms. Synchrony indices for all experiments were averaged across time frames and across tasks. When reporting the results for the asymmetric synchrony measures, we will use J-SESM-FM instead of J-SESM-12, as defined in (8), that captures the extent to which the atoms selected to represent the male EDA can be used to represent the female EDA. Similarly we will employ J-SESM-MF instead of J-SESM-21, as defined in (9).

Results suggest that the joint SESM indices depict significant differences across tasks for both datasets, while this effect is not significant for the simple SESM scores (Table 1). For the married couples’ dataset, we further notice an increasing trend of the joint SESM across tasks of increasing emotional intensity (Fig. 2b). Similar patterns apply for the young couples (Fig. 2a). However, in the young couples’ dataset the relaxation task depicted higher SESM values compared to the discussions. This can be attributed to the distinct nature of baseline procedures between the two datasets, since the first involves a relaxation through a video stimuli watched at the same time by both partners, while the second contains rest periods during which the two partners were not engaged in any activity. Therefore the increased synchrony of young couples during the relaxation task might be due to the fact that they are responding to the

TABLE 1. Repeated-measures ANOVA for overall significant differences of Sparse EDA Synchrony Measures (SESM) across tasks.

Young couples’ interactions			
EDA Representation	Synchrony Measure	F-statistic	P-value
Single	S-SESM-DTW	F(4,175)=1.67	.16
	S-SESM-L2	F(4,175)=1.47	.12
Joint	J-SESM	F(4,175)=24.12	<.01
	J-SESM-FM	F(4,175)=14.17	<.01
	J-SESM-MF	F(4,175)=20.31	<.01
Married couples’ interactions			
EDA Representation	Synchrony Measure	F-statistic	P-value
Single	S-SESM-DTW	F(5,180)=0.4	.85
	S-SESM-L2	F(5,180)=0.35	.88
Joint	J-SESM	F(5,180)=5.56	<.01
	J-SESM-FM	F(5,180)=2.32	.05
	J-SESM-MF	F(5,180)=6.08	<.01

TABLE 2. Pearson’s correlation between single/joint-representation sparse EDA synchrony measures (S-SESM/J-SESM) and self-reported attachment ratings (\*,† denote  $p < 0.05, 0.1$ ).

Young couples’ interactions			
EDA Representation	Synchrony Measure	Avoidance	Anxiety
Single	S-SESM-DTW	.29 <sup>†</sup>	.07
	S-SESM-L2	-.43*	-.43*
Joint	J-SESM	.11	.36*
	J-SESM-FM	.13	.33 <sup>†</sup>
	J-SESM-MF	.10	.27
Married couples’ interactions			
EDA Representation	Synchrony Measure	Avoidance	Anxiety
Single	S-SESM-DTW	-.03	.08
	S-SESM-L2	.14	.10
Joint	J-SESM	.43*	.43*
	J-SESM-FM	.39*	.51*
	J-SESM-MF	.41*	.46*

same stimuli, which causes a steep physiological decrease for both and therefore high similarity in their EDA signals.

Statistical tests and regression tasks further indicate the association of the proposed synchrony measures with the self-reported attachment scores. Joint SESM indices appear to be significant predictors of attachment (Table 2), suggesting the advantage of simultaneously representing two streams of data for the task of interest. Anxious attachment appeared to be more strongly associated with synchrony than the avoidance measures (Tables 2, 3), a finding consistent with previous work [12].

## 6. Conclusion

We propose a framework to quantify EDA synchrony through the use of sparse decomposition techniques with appropriately designed signal-specific parametric dictionaries. SESM indices are derived either through the distance between the parametric spaces of the two signals or through their joint representation error. Statistical analysis and regression experiments indicate that SESM scores differ across tasks of various emotional intensity and are associated to relationship attachment patterns.

Future work will expand the proposed measures to include more physiological signals, such as the ECG, and will

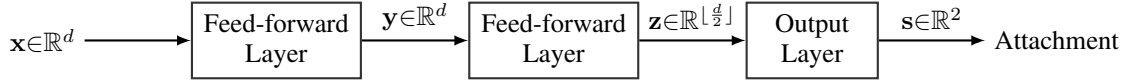


Figure 1. Schematic representation of a deep neural network structure that performs non-linear regression for predicting the attachment scores based on sparse EDA synchrony measures (SESM).

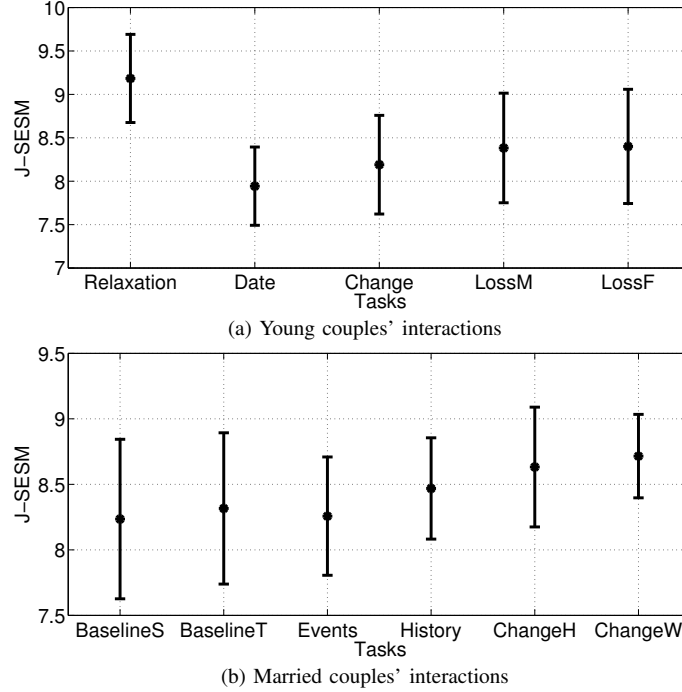


Figure 2. Joint Sparse EDA Synchrony Measure (J-SESM) across tasks. Error bars represent one standard deviation distance from the mean.

TABLE 3. Pearson's correlation between ground-truth and predicted attachment ratings using sparse EDA synchrony measure (SESM) features in regression experiments (\*, † denote  $p < 0.05$ ,  $0.1$ ).

Young couples' interactions			
EDA Representation	Synchrony Vector	Avoidance	Anxiety
Single	S-SESM	.34*	.12
Joint	J-SESM	.24	.1
Single & Joint	S-SESM & J-SESM	.37*	.38*

Married couples' interactions			
EDA Representation	Synchrony Vector	Avoidance	Anxiety
Single	S-SESM	.32†	.30
Joint	J-SESM	.1	.35†
Single & Joint	S-SESM & J-SESM	.36†	.41*

examine how the current findings can be translated to ambulatory data collected from wearable devices in everyday life. Another future direction includes exploring time dynamics of physiological synchrony as a function of contextual and relationship-dependent factors.

## References

- [1] L.K. Miles, L.K. Nind, and C.N. Macrae, "The rhythm of rapport: Interpersonal synchrony and social perception," *Journal of experimental social psychology*, vol. 45, no. 3, pp. 585–589, 2009.
- [2] L.K. Cirelli, K.M. Einarson, and L.J. Trainor, "Interpersonal synchrony increases prosocial behavior in infants," *Developmental Science*, vol. 17, no. 6, pp. 1003–1011, 2014.
- [3] R. Feldman, "Parent-Infant Synchrony Biological Foundations and Developmental Outcomes," *Current directions in psychological science*, vol. 16, no. 6, pp. 340–345, 2007.
- [4] D. Saxbe and R.L. Repetti, "For better or worse? Coregulation of couples' cortisol levels and mood states," *Journal of personality and social psychology*, vol. 98, no. 1, pp. 92, 2010.
- [5] A. Karvonen, V.L. Kykryri, J. Kaartinen, M. Penttonen, and J. Seikkula, "Sympathetic nervous system synchrony in couple therapy," *Journal of marital and family therapy*, 2016.
- [6] A.C. Timmons, G. Margolin, and D.E. Saxbe, "Physiological linkage in couples and its implications for individual and interpersonal functioning: A literature review," *J. Fam. Psychol.*, vol. 29, no. 720, pp. 10–1037, 2015.
- [7] R. W. Levenson and J.M. Gottman, "Marital Interaction: Physiological Linkage and Affective Exchange," *Journal of personality and social psychology*, vol. 45, no. 3, pp. 587–597, 1983.
- [8] J.L. Helm, D. Sbarra, and E. Ferrer, "Assessing cross-partner associations in physiological responses via coupled oscillator models," *Emotion*, vol. 12, no. 4, pp. 748, 2012.
- [9] E. Ferrer and J.L. Helm, "Dynamical systems modeling of physiological coregulation in dyadic interactions," *International Journal of Psychophysiology*, vol. 88, no. 3, pp. 296–308, 2013.
- [10] S. Liu, M.J. Rovine, Cousino K.L., and D.M. Almeida, "Synchrony of diurnal cortisol pattern in couples," *Journal of Family Psychology*, vol. 27, no. 4, pp. 579, 2013.

- [11] A.C. Timmons, T. Chaspari, S.C. Han, L. Perrone, S.S. Narayanan, and G. Margolin, "Using multimodal wearable technology to detect conflict among couples," *IEEE Computer*, vol. 50, no. 3, pp. 50–59, 2017.
- [12] A.C. Timmons, Baucom B.R., Han S.C., Perrone L., T. Chaspari, S.S. Narayanan, and G. Margolin, "New frontiers in ambulatory assessment: Big data methods for capturing couples' emotions, vocalizations, and physiology in daily life," *Social Psychological and Personality Science*, 2017.
- [13] R.G. Reed, A.K. Randall, J.H. Post, and E.A. Butler, "Partner influence and in-phase versus anti-phase physiological linkage in romantic couples," *International Journal of Psychophysiology*, vol. 88, no. 3, pp. 309–316, 2013.
- [14] R. Fusaroli, I. Konvalinka, and S. Wallot, "Analyzing social interactions: the promises and challenges of using cross recurrence quantification analysis," in *Translational recurrences*, pp. 137–155. Springer, 2014.
- [15] K. Fujiwara and I. Daibo, "Evaluating interpersonal synchrony: Wavelet transform toward an unstructured conversation," *Frontiers in psychology*, vol. 7, 2016.
- [16] E. Delaherche, M. Chetouani, A. Mahdhaoui, C. Saint-Georges, S. Viaux, and D. Cohen, "Interpersonal synchrony: A survey of evaluation methods across disciplines," *IEEE Transactions on Affective Computing*, vol. 3, no. 3, pp. 349–365, 2012.
- [17] T. Chaspari, A. Tsiartas, I. L. Stein, Cermak S. A., and S. Narayanan, "Sparse Representation of Electrodermal Activity with Knowledge-Driven Dictionaries," *IEEE Transactions on Biomedical Engineering*, vol. 62, no. 3, pp. 960–971, 2015.
- [18] R. Balasubramanian, T. Chaspari, and S.S. Narayanan, "A knowledge-driven framework for ecg representation and interpretation for wearable applications," in *Proc. IEEE International Conference on Acoustics, Speech and Signal Processing (ICASSP)*, 2017, pp. –.
- [19] Y.C. Pati, R. Ramin, and P.S. Krishnaprasad, "Orthogonal matching pursuit: Recursive function approximation with applications to wavelet decomposition," *Conference on Signals, Systems and Computers*, 1993.
- [20] G. Davis, S.G. Mallat, and M. Avellaneda, "Adaptive greedy approximations," *Constructive Approximation*, vol. 13, no. 1, pp. 57–98, 1997.
- [21] J.A. Tropp, "Greed is good: Algorithmic results for sparse approximation," *IEEE Transactions on Information Theory*, vol. 50, no. 10, pp. 2231–2242, 2004.
- [22] J.A. Tropp and A.C. Gilbert, "Signal recovery from random measurements via orthogonal matching pursuit," *IEEE Transactions on Information Theory*, vol. 53, no. 12, pp. 4655–4666, 2007.
- [23] M.E. Dawson, A.M. Schell, and D.L. Fillion, "The Electrodermal System," in *Handbook of psychophysiology*, J.T. Cacioppo, L.G. Tassinari, and G.G. Berntson, Eds., pp. 159–181. New York: Cambridge University Press, 3rd edition, 2007.
- [24] W. Boucsein, *Electrodermal activity*, Springer, New York, NY, 2012.
- [25] J.A. Tropp, A.C. Gilbert, and M.J. Strauss, "Simultaneous sparse approximation via greedy pursuit," in *Acoustics, Speech, and Signal Processing, 2005. Proceedings.(ICASSP'05). IEEE International Conference on*, 2005, vol. 5, pp. 721–724.
- [26] T. Chaspari, B. Baucom, A.C. Timmons, A. Tsiartas, L. B. Del Piero, K.J.W. Baucom, P. Georgiou, G. Margolin, and S.S. Narayanan, "Quantifying eda synchrony through joint sparse representation: A case-study of couples' interactions," in *Proc. IEEE International Conference on Acoustics, Speech and Signal Processing (ICASSP)*, 2015, pp. 817–821.
- [27] R Chris Fraley, Niels G Waller, and Kelly A Brennan, "An item response theory analysis of self-report measures of adult attachment," *Journal of personality and social psychology*, vol. 78, no. 2, pp. 350, 2000.
- [28] J.A. Simpson, W.S. Rholes, and D. Phillips, "Conflict in close relationships: an attachment perspective," *Journal of personality and social psychology*, vol. 71, no. 5, pp. 899–914, 1996.
- [29] D. Kingma and J. Ba, "Adam: A method for stochastic optimization," *arXiv preprint arXiv:1412.6980*, 2014.
- [30] F. Chollet, "Keras," <https://github.com/fchollet/keras>, 2015.
- [31] F. Bastien, P. Lamblin, R. Pascanu, J. Bergstra, I. Goodfellow, A. Bergeron, N. Bouchard, D. Warde-Farley, and Y. Bengio, "Theano: new features and speed improvements," *arXiv preprint arXiv:1211.5590*, 2012.